Polymer Testing 116 (2022) 107760

Contents lists available at ScienceDirect

Polymer Testing

journal homepage: www.elsevier.com/locate/polytest

Long-term antimicrobial effect of polylactide-based composites suitable for biomedical use

Kateřina Škrlová [a,b], Zuzana Rybková [c], Tereza Stachurová [c], Jakub Zagora [a,b], Kateřina Malachová [c], Dagmar Měřinská [d], Roman Gabor [a], Miroslav Havlíček [e], Alexandra Muñoz-Bonilla [f], Marta Fernández-García [f], Daniela Plachá [a,g,*]

[a] Nanotechnology Centre, CEET, VSB – Technical University of Ostrava, 17. listopadu 2172/15, 708 00, Ostrava-Poruba, Czech Republic
[b] Center of Advanced Innovation Technologies, VSB – Technical University of Ostrava, 17. listopadu 2172/15, 708 00, Ostrava-Poruba, Czech Republic
[c] Department of Biology and Ecology, Faculty of Science, University of Ostrava, Chittussiho 10, 710 00, Ostrava, Czech Republic
[d] Faculty of Technology, Tomas Bata University in Zlín, Vavrečkova 275, 760 01, Zlín, Czech Republic
[e] Medin,a.s., Nové Město na Moravě, Czech Republic
[f] Institute of Polymer Science and Technology (ICTP-CSIC), Juan de la Cierva 3, 28006, Madrid, Spain
[g] ENET Centre, CEET, VSB – Technical University of Ostrava, 17. listopadu 2172/15, 708 00, Ostrava-Poruba, Czech Republic

ARTICLE INFO

Keywords:
Polylactide
Polymer composites
Antimicrobial effect
Silver
HDTMA
HDP
Stents

ABSTRACT

This work deals with the preparation and characterization of antimicrobial polymeric composite materials based on polylactide, which is currently widely investigated to produce temporary implants. Polylactide was blended with antimicrobial fillers: silver, hexadecylpyridinium or hexadecyltrimethylammonium bromides anchored on vermiculite or graphene oxide matrices in an amount of 1% wt. The prepared samples were characterized by conventional methods, further they were exposed to degradation tests in physiological saline conditions and characterized for their antimicrobial properties using common pathogen microorganisms. It has been proven that the prepared polylactide composites change their antimicrobial effects after being in physiological saline of pH 7 and 9 for 0–6 months. The weight of the composites changed by about 10%, and antimicrobial properties were growing over time. The effectiveness of the composites was confirmed for 6 months at minimum. Therefore, they are suitable for the preparation of temporary stents, catheters or implants suitable for fracture fixation.

1. Introduction

Polylactide (PLA) is a biobased hydrophobic polymer made from renewable resources and one of the most stable biodegradable polymeric materials currently used for many applications due to its unique properties such as excellent biocompatibility, thermoplastic processability and environmental friendliness. Its properties are comparable to petroleum-based polymers, especially in high strength. It can be an alternative to synthetic and non-degradable materials for some applications, reducing reliance on petroleum-based polymers [1–4].

Because PLA is biocompatible with human tissue, it is suitable for the manufacture of implants, sutures, stents, patches, drug delivery systems, scaffolds for tissue growth, and other medical products [1,2]. It can be easily modified using fillers for preparation of (nano)composites that acquire new physical, mechanical or antimicrobial properties depending on the type of filler used [3,5]. Since PLA is (bio)degradable, the fillers can be released into the environment when they decompose, which can be an advantage for medical use, as it can help relieve pain or treat health problems right at the site of application [3,4,6].

As previously mentioned, PLA can be used to produce medical stents. The stents are widely used to restore patency in almost all tubular organs in the human body, such as blood vessels, oesophagus, duodenum, gallbladder, pancreas, urethral or prostatic tracts. Various diseases can cause narrowing or clogging of these tubular organs preventing proper flow of blood and other body fluids. This is serious and very painful complication. An endoscopically inserted stent can restore the passage of the tubular organ and solve the problem. In addition, the stent can have a drug incorporated that is gradually released at the site of the stent insertion site, so the treatment itself can take place here [3,7–10].

Stents can be made of three types of materials: (i) metals, (ii)

Abbreviations: HDP, hexadecylpyridinium cations; HDTMA, hexadecyltrimethylammonium cations; PLA, polylactide.

* Corresponding author. Nanotechnology Centre, CEET, VSB - Technical University of Ostrava, 17. listopadu 2172/15, 708 00, Ostrava-Poruba, Czech Republic.
E-mail address: daniela.placha@vsb.cz (D. Plachá).

https://doi.org/10.1016/j.polymertesting.2022.107760
Received 22 April 2022; Received in revised form 21 July 2022; Accepted 27 August 2022
Available online 5 September 2022

permanent polymeric materials and iii) biodegradable polymeric materials. The advantage of biodegradable polymer stents compared to permanent polymer or metals stents is that they do not have to be surgically removed from the patient's body after treatment as they gradually break down into low-molecular weight substances that are further metabolized [11–14].

A major complication when using a stent in the human body is the formation of a microbial biofilm on its walls, which is made up of the residues of body fluids and microorganisms found in the human body. Bacteria and yeasts that form a biofilm, e.g. *Escherichia coli, Staphylococcus aureus, Pseudomonas aeruginosa, Streptococcus salivarius* and *Candida albicans,* can cause serious infection that can lead to the patient's death [15,16]. *E. coli* is a gram-negative bacterium commonly found in the large and small intestine. If it occurs in other parts of the body, it can cause infectious diseases. *S. aureus* is a gram-positive bacterium living on human skin and mucous membranes. *S. salivarius* is a gram-positive bacterium that is part of the human microflora of the skin and mucous membranes [17]. *P. aeruginosa* is gram-negative bacteria that causes infections in hospitalized patients (e.g., pneumonia, sepsis, urinary tract infections). The pathogenic yeast *C. albicans* is present on the skin and mucous membranes and causes candidiasis, endocarditis, bloodstream infections [18].

To prevent microbial attack and consequent biofilm growth, the polymeric composites containing antimicrobial fillers can be used for stents production [3,5,19]. Many substances with confirmed antimicrobial effects, among them carbon nanomaterials, metal nanoparticles, their oxides or ionic forms, such as silver, copper, iron oxides, ZnO, TiO_2, CaO, quaternary ammonium salts and other organic cations, chitosan, essential oils, can be applied as fillers [20–35]. A number of research works have focused on studying PLA with antimicrobial properties through surface modification or composite preparation using an antimicrobial agent or a combination of them. Fillers were used in different amounts for different polymers and the resulting composites were tested on different microbial tests [23,36,37].

In the case of anchoring the filler only on the surface of the materials, the antimicrobial effect may be only short-term, as the fillers may leak into the environment. If the filler is embedded in the matrix, it may be inaccessible to microorganisms and the antimicrobial effect may not be manifested. In this case, the degradability of PLA can be a very advantageous property bringing the long-term inhibitory effect of PLA composites. PLA itself degrades after a few months under the action of moisture or biological agents, mainly by hydrolysis of esters bonds to form water-soluble oligomers and monomers or even CO_2 and water [38–40]. It can be degraded by a number of different mechanisms including hydrolytic, oxidative, thermal, microbial, enzymatic or photodegradative and chemical processes. Hydrolysis of PLA has been described in a number of research works explaining that the rate of degradation depends on PLA isomer composition, degree of crystallinity, molecular weight, hydrolysis temperature, pH, oxygen, shape and size of materials, and others. It is also well known that hydrolysis occurs more readily in the amorphous regions of PLA [41]. Two opposing mechanisms can take place during hydrolysis: heterogeneous or surface reactions and homogeneous or bulk erosion [39,41]. During a surface erosion, only the surface of the polymer undergoes degradation and erosion, leaving the bulk intact. In contrast, if bulk degradation occurs, the rate of degradation is essentially the same at every point in the matrix [42]. The acidity or alkalinity of the medium is an important parameter affecting the hydrolysis of PLA, since H^+ or OH^- ions catalyze the cleavage of ester groups [43]. It is well known that fillers can modify the degradation properties of PLA, e.g. as clay minerals accelerate hydrolytic degradation by improving the hydrophilicity of the material [1].

The aim of this study is the development of composite materials based on polylactide, which could be suitable for biomedical applications, especially for production of stents used in the bile ducts. The polylactide was enriched with fillers based on graphene oxide and vermiculite, which were modified with antimicrobial substances such as silver, hexadecylpyridinium or hexadecyltrimethylamonium cations. Graphene oxide and vermiculite served as a carrier without any antimicrobial effect, since the use of antimicrobial components without a carrier would impair the mechanical properties of the polymer matrix. The prepared composites were immersed in buffer solutions of pH 7 (to simulate the environment in most tubular organs of the human body) and 9 (to simulate the environment in the bile ducts) for six months, and their antimicrobial effects on selected microorganisms, bacteria and yeast, were gradually tested. It was based on the hypothesis that when storing composites at the above-named pHs, there will be a gradual degradation of these composites and the associated gradual release of antimicrobial fillers into the environment. As a result, there will be a long-term inhibition of bacteria that could participate in the formation of biofilm on the surface of the stents.

2. Materials and methods

2.1. Materials

Poly(lactic acid) (PLA), IngeoTM 4032D, was supplied by RESINEX Czech Republic s.r.o. The material has a density of 1.24 g/cm^3, glass transition temperature (Tg) of 59 °C and melting point of 160 °C. The molecular weight (Mw) of the PLA is 182,000 g/mol as was determined by gel permeation chromatography.

Graphene oxide (GO) was prepared by a modified Hummers' method using concentrated H_2SO_4, $KMnO_4$, graphite flakes, and concentrated H_2O_2 according to the literature [25]. All compounds needed for its preparation were supplied by Sigma-Aldrich, Co. For clay fillers, vermiculite (VMT) Palabora from Southern Africa (GRENA a.s.) with a cation exchange CEC value of 89 cmol$^{(+)}$/kg was used. Vermiculite was modified to sodium form using NaCl (Sigma-Aldrich, Co.) for better cation exchange. The sodium form of vermiculite was denoted as Na-VMT. Fillers were modified using $AgNO_3$ (>99%), hexadecylpyridinium cations (HDP), hexadecyltrimethylamonium cations (HDTMA) [26–28]. All compounds were supplied by Sigma-Aldrich, Co.

2.2. Microbial strains

Bacterial gram-negative (G-) strains *Escherichia coli* (CCM 3988) and *Pseudomonas aeruginosa* (CCM 1960), gram-positive (G+) strains *Staphylococcus aureus* (CCM 4223), *Streptococcus salivarius* (CCM 4046), and yeast strain *Candida albicans* (CCM 8186) were obtained from the Czech Collection of Microorganisms (CCM, Brno, Czech Republic). The microbial strains represent a group of potential pathogens causing urinary tract diseases, endocarditis, nosocomial infections and skin diseases [44]. Bacteria were cultivated 24 h at 37 °C on the Nutrient agar plates (HiMedia, India). Yeast was cultivated 48 h at 28 °C on the plates with the Glucose Peptone Yeast extract (GPY) agar (glucose 40 g L^{-1}, peptone 5 g L^{-1}, yeast extract 5 g L^{-1}, agar 15 g L^{-1}, HiMedia, India).

2.3. Preparation of antimicrobial fillers

Four antimicrobial fillers were prepared. The first graphene oxide filler with Ag was prepared as follows: 0.1 g of GO was mixed with 1 g of $AgNO_3$ (> 99%) in a volume of 100 mL of demineralized water. GO was dispersed together with $AgNO_3$ (the concentration of $AgNO_3$ was 0.059 mol L^{-1}) in demineralized water using a shaker for 24 h. The entire mixture was then allowed to stand until a deposit formed at the bottom of the beaker. The upper layer of demineralized water was poured off, pure demineralized water was added, the mixture was shaken briefly, and a precipitate was allowed to form again. The mixture was then washed several times and dried at 60 °C to a powder. A second filler based on silver modified vermiculite was prepared as follows: 8.4 g of $AgNO_3$ and 50 mL of demineralized water were used to prepare a 1 mol L^{-1} $AgNO_3$ solution, which was then mixed with 5 g of Na-VMT at 80 °C

for 3 h. The mixture was then washed several times with demineralized water and dried to the powder. The third and fourth fillers were Na-VMT modified with HDP and HDTMA cations, which were prepared according to previous studies [25–28]. The prepared fillers were denoted as GO + Ag, VMT + Ag, VMT + HDP, and VMT + HDTMA.

2.4. Preparation of antimicrobial polymer composites

Pure polylactide and polylactide composite films were prepared as follows: 1) PLA pellets were introduced into a polymer extruder (Thermo Scientific™ HAAKE™ MiniLab 3 Micro Compounder) at 160 °C, 100 rpm and for 5 min. After this process, the extruded PLA was pressed at 200 °C for 5 min. This polylactide film was indicated as PLA. 2) PLA composite films were prepared in the same manner as neat PLA; however, 1 wt% of filler was added to the extruder. The filler content was chosen based on our experiments showing the lowest filler content that has an effective antimicrobial effect. PLA composites films were denoted as PLA + GO + Ag, PLA + VMT + Ag, PLA + VMT + HDP, PLA + VMT + HDTMA (see Table 1).

2.5. Methods of characterization

Determination of the PLA average number molecular weight (MW) by gel permeation chromatography (GPC) was performed using an Agilent GPC PL-GPC 220 instrument under the following conditions: columns used: PL gel MIXED-A (300 × 7.8 mm, 20 μm) + MIXED-B (300 × 7.8 mm, 10 μm) + MIXED-D (300 × 7.8 mm, 5 μm), mobile phase: tetrahydrofuran (stabilized - BHT), temperature: 40 °C, injection volume: 100 μL, flow rate: 1 mL/min, detectors: RI detector, viscometric detector, measured data were processed using Cirrus Software. The determination of the Ag content in the fillers by inductively coupled plasma atomic emission spectrometry (ICP-AES) was performed on a SpectroCiros Vision instrument. Determination of organic carbon content in modified vermiculites was performed using a LECO RC612 phase carbon analyzer with an infrared detector; a temperature program in the range of 100–1100 °C with an increase of 0.9 °C/s was used in the analysis. A 10 mg sample was burned in a stream of oxygen, the resulting products were determined in the detector as CO_2. Fourier transform infrared spectroscopy (FTIR) for the characterization of fillers was performed using a Nicolet iS50 FTIR spectrometer (ThermoScientific, USA) with a diamond crystal, in the range of 4000-400 cm^{-1}, by the attenuated total reflection (ATR) method at a spectral resolution of 0.4 cm^{-1}. The Raman spectrum of graphene oxide was measured using a DXR Raman Microscope Dispersion Raman Microscope (Thermoscientific, USA) at a wavelength of 532 nm. Diffraction (XRD) recordings were taken on a RIGAKU Miniflex600 X-ray diffractometer (Cu-lamp, lamp wavelength λ = 0.15406 nm, scintillation detector, NiK_β filter, Bragg-Brentan arrangement). The samples were placed in a standard holder, measurement conditions: 40 kV, 15 mA, measurement range 2–70° 2theta and 1–70° 2theta for organically modified vermiculites, measurement rate 2.4°/min. Thermogravimetric analysis (TGA) of the polymer and polymer composites was performed to determine their thermo-stability. The measurements were performed on a SETSYS Evolution (Setaram Instrumentation). Samples (~10 mg) were heated in the temperature range 20–1000 °C with a heating rate of 10 °C/min in crucibles made of α-Al_2O_3 in a dynamic atmosphere of argon with a flow rate of 100 cm^3/min. Analysis of polymers and polymer composites by differential scanning calorimetry (DSC) was performed on a Setaram Instrumentation DSC131 EVO differential scanning calorimeter equipment, measuring in the temperature range 0–200 °C with a programmed temperature increase of 5 °C/min. Analysis by optical microscopy was performed on a VHX-2000 Light Digital Microscope (Keyence Corporation, Japan). To determine the detailed analysis of particles, a scanning electron microscope (SEM) JEOL JSM-7610F Plus (JEOL, Japan) with an auto emission source was used. The samples were monitored at an accelerating voltage of 15 keV using secondary electron detection. Samples were analyzed by energy dispersive X-ray spectroscopy: EDX ULTIM MAX 65 mm^2, Oxford Instruments. All graphs were processed in the program Origin 2019b (64-bit), 9.6.5.169 (Academic).

Table 1
Prepared PLA composites and filler explanation.

Sample identification	Filler	Filler content in PLA (antimicrobial agent content in the filler)
PLA	No filler	0 wt% (0 wt%)
PLA + GO + Ag	Ag anchored on graphene oxide	1 wt% (61 wt%)
PLA + VMT + Ag	Ag anchored on vermiculite	1 wt% (9 wt%)
PLA + VMT + HDP	Vermiculite modified by hexadecylpyridinium cations	1 wt% (20 wt%)[a]
PLA + VMT + HDTMA	Vermiculite modified by hexadecyltrimethylammonium cations	1 wt% (24 wt%)[a]

[a] Expressed as organic carbon content in the filler.

2.5.1. Antimicrobial tests

Antimicrobial effects of the fillers were performed by the broth microdilution method and disk diffusion method [45,46]. The microdilution method was used for the determining of minimum inhibition concentrations (MIC) of the tested fillers. Bacterial strains were inoculated into 10 mL of Mueller-Hinton Broth (MHB, HiMedia, India) and cultivated overnight at 37 °C. Yeast strain was inoculated into 10 mL of extract GPY and cultivated overnight at 28 °C. Overnight microbial strains were diluted with a sterile 0.15 mol/L saline solution to the density of a 0.5 McFarland (McF) unit (Densilameter, ErbaLachema, Czech Republic). The samples were tested in a concentration range of 0.1–500 μg/mL. A sample volume of 20 μL, 160 μL of MHB or GPY and 20 μL of microorganism suspension (0.5 McF) were added to each wells of 96-well microtiter plate (Anicrin S.r.l., Italy). The microtiter plates were incubated at 37 °C (bacterial strains) or 28 °C (yeast strain) at shaking 120 rpm (ELMI orbital shaker DOC-20l, Latvia) for 24 h. After this incubation, the bacteria were transferred using the inoculate hedgehog (ErbaLachema, Czech Republic) to new microtiter plates with 200 μL of MHB or GPY per well and were incubated 24 h at 37 °C or 28 °C. The presence of turbidity was detected spectrophotometrically (Epoch microplate spectrophotometer, BioTek, USA) at a wavelength of 620 nm. The MIC was recorded as the lowest concentration of the sample that inhibits growth of microorganism.

Antimicrobial activities of the fillers were also evaluated by the disk diffusion method [47]. Mueller-Hinton Agar plates (MHA, HiMedia, India) for bacteria and GPY agar plates for yeast were inoculated with the 0.5 McF microbial suspension. Four sterile discs of filter paper (6 × 6 mm) were applied to the surface of the inoculated agar plate within 15 min of inoculation. The sample was applied to the four discs in the concentration 37, 74, 111 and 148 μg/disc. The MHA and GPY agar plates with the discs were incubated 24 h at 37 °C or 28 °C. After the incubation, the inhibition zone diameters were measured.

2.5.2. Dynamic antimicrobial tests at different pHs

The antimicrobial effectiveness of PLA composites immersed in physiological pHs during different time periods was evaluated by disc diffusion using: 6 × 6 mm disks. pH 9 was selected according to the pH value occurring in the gallbladder and bile duct, while pH 7 was used as a control neutral value. After the required time (0, 1, 2, 3 and 6 months), some discs were removed from saline, dried at 37 °C and subjected to antimicrobial testing and microscopic characterization.

2.5.3. Statistical analysis

Each experiment was done in, at least, five replicates. One Way Analysis Data was represented as mean SD. One-Way ANOVA was used to evaluate any significant difference between the MIC values of the

composites containing the test reagents and their respective controls. Differences in the antimicrobial activity of immersed PLA composites at pH 7 and pH 9 and results depending on time were also evaluated [48]. $p < 0.05$ was considered as statistically significant. All statistical analyses were executed using the program R (R Core Team, 2016; version 3.4.0).

3. Results and discussion

The discussion of the achieved results is divided into two parts: 1) characterization of fillers and 2) characterization of composites.

3.1. Characterizations of fillers

ICP-AES, XRD and SEM methods were used for characterization of Ag-bearing fillers, and total carbon content (TOC), FTIR, XRD and SEM measurements were used to characterize the organically modified vermiculites.

The Ag content in the GO + Ag and VMT + Ag fillers was determined using ICP-AES, where 61.0 ± 6.1 wt% and 9.0 ± 0.9 wt% of Ag was determined, respectively. The difference in the Ag content corresponds to the different methods of fillers preparation, when then amount of Ag^+ (see Part 1.3.) was used in the ratio Ag^+/GO 6.35 and Ag^+/VMT 1.07, respectively. However, measuring the total amount of Ag does not provide any information to distinguish between ionic or molecular silver; for this reason, XRD analysis was performed. The analysis shows (shown below) the diffraction pattern of the prepared GO + Ag, in the 2θ range from 5 to 70°. Diffraction peaks at 2θ 39.1°, 43.4° and 64.8° were observed in the pattern, which can be attributed to Ag nanoparticles. According to earlier studies, the sharp crystalline peaks correspond to (111), (200), and (220) reflection planes of crystalline Ag NPs with a face-centered cubic structure [49]. It has also been demonstrated that GO alone can transform $AgNO_3$ and act as a substrate for the formation of Ag nanoparticles to obtain GO + Ag nanocomposites [50]. The remaining peaks indicate the predominant presence of Ag^+ ions in $AgNO_3$ and trace amounts of Ag_2O. The peak characteristic for GO at 12.8° disappeared probably because the regular stack of GO was destroyed by the intercalation of Ag particles in the GO + Ag composite or it is shaded by the high amount of $AgNO_3$ deposited on the surface of GO.

The diffraction pattern of VMT + Ag was measured in the same range as before. Diffraction peaks characteristic of the Na form of vermiculite were observed at 2θ 7.8° (d = 11.4 Å) and at 19.5° (d = 4.5 Å). The peaks at 38.2°, 44.6° and 60.1° were characteristic of the presence of Ag nanoparticles. It follows that while GO carries an unspecified mixture of Ag particles, Ag^+ ions and Ag_2O, VMT + Ag, prepared without any other reagents, mainly contains Ag nanoparticles.

The morphology surface visualization was done using scanning electron microscopy with energy dispersive X-ray spectroscopy (EDX). In the case of the GO + Ag, inconsistently distributed particles of various irregular shapes and sizes are evident (Fig. 1a). Chemical composition analysis using EDX analysis (see Table S1) determined the presence of silver (43 wt%) on the surface of the composite filler as well as the presence of nitrogen corresponding to nitrate. To determine the Ag coverage, mapping of the GO + Ag surface was performed (Fig. 1b). The surface of the composite was found to be covered with a relatively continuous but uneven layer of Ag (green color). The presence of nitrogen (yellow/orange color) is slightly obvious. The findings from the XRD analysis were thus confirmed, the GO + Ag filler contains Ag in the form of Ag^+ ($AgNO_3$), Ag_2O and Ag nanoparticles.

The SEM visualization of the VMT + Ag filler (see Table S2) also showed clay particles with different shapes and sizes (Fig. 1c). Likewise,

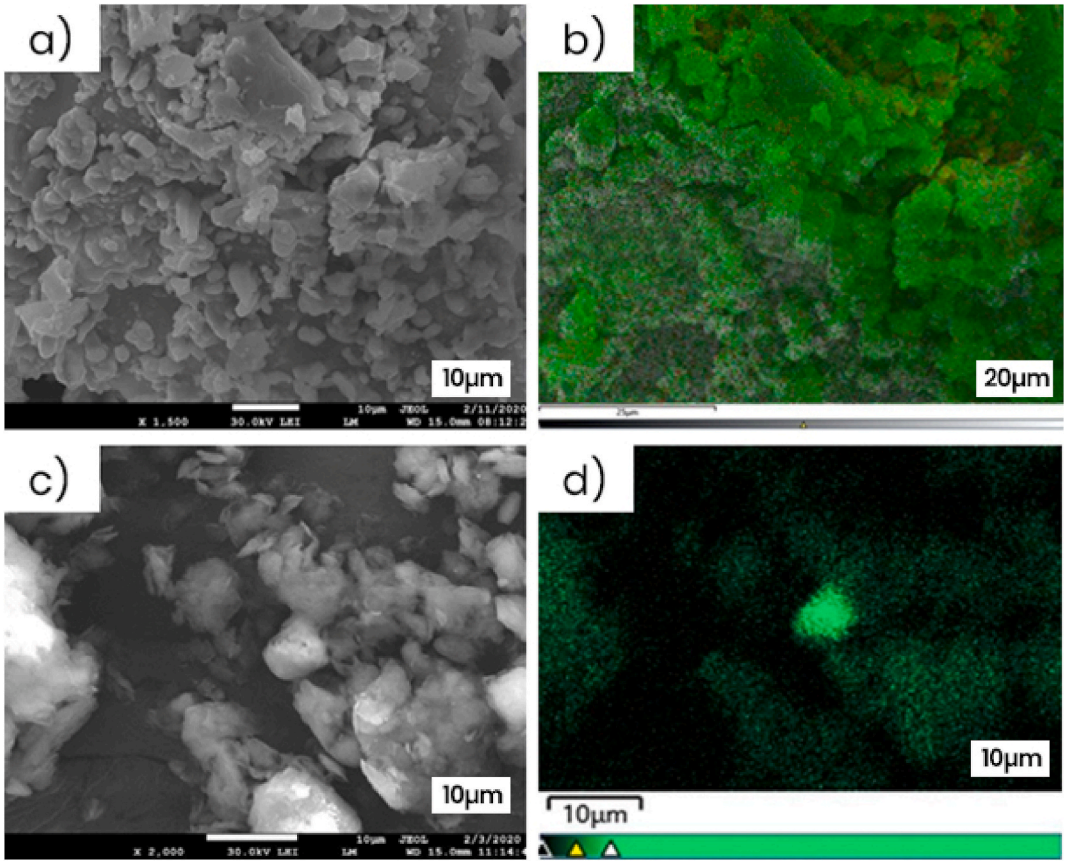

Fig. 1. Surface mapping for the presence of Ag (green) by SEM/EDX method, a) and b) GO + Ag, c) and d) VMT + Ag, a) and c) in scale of 10 μm. (For interpretation of the references to color in this figure legend, the reader is referred to the Web version of this article.)

the presence of Ag was confirmed by EDX analysis (4.3 wt %), while nitrogen was not identified. Thus, it is assumed that the VMT + Ag filler is covered mainly by Ag nanoparticles, as confirmed by mapping (Fig. 1d). EDX analysis was also performed for VMT + HDP (see Table S3) and VMT + HDTMA (see Table S4) samples.

The TOC analysis shows the carbon content in fully inorganic vermiculite after organic modification, confirming successful modification. The VTM + HDP and VMT + HDTMA analyses showed that the carbon content increased by 20 wt% (about 90% of the original inorganic cations in the vermiculite interlayer were exchanged) and by 24 wt% (120% of the inorganic cations were exchanged), respectively [26,27].

FTIR and XRD analysis are among the other tools enabling the confirmation of the presence of organic functional groups in organically modified vermiculites [26–28]. The FTIR spectra of both fillers are displayed in Fig. S1. Briefly, the identified absorption bands confirmed the presence of HDP or HDTMA cations in the vermiculite structure. First, intense bands in the region of 2916 and 2851 cm^{-1}, which are characteristic for valence asymmetric and symmetric vibrations of C–H bonds in the $–CH_2$ group. Furthermore, the spectrum shows a small band in the region of 2952 cm^{-1}, which corresponds to the valence C–H vibrations of the $–CH_3$ group. More information about FTIR analyses is presented in Supplement.

Fig. 2 shows the XRD patterns of all modified fillers. The XRD patterns of GO + Ag and modified VMT was described above. The XRD patterns of neat GO, raw VMT and Na-VMT are given in the supplement, Fig. S2. The XRD pattern of the prepared VMT + HDP was measured in the 2θ range from 1° to 70°. Confirming the successful intercalation of HDP into the vermiculite structure is the diffraction peak at 1.8° corresponding to the interlayer distance d = 50.3 Å (5.3 nm) (see inset in Fig. 2). This significant increase in the interlayer distance compared to the original layered distance of 12.2 Å is caused by the intercalation of HDP into the vermiculite structure [26]. The diffraction peaks observed at 7.3° and 8.9°, d = 10.0 Å (1.0 nm) indicate an uneven intercalation of HDP into the vermiculite structure. The diffraction pattern of the VMT + HDTMA filler also shows a diffraction peak at 1.9° corresponding to an interlayer distance of d = 47.1 Å (4.7 nm) [27] confirming that the HDTMA cations are intercalated into the vermiculite interlayer. Other diffraction peaks were observed at 3.6° with d = 24.8 Å (2.5 nm) and 7.0°, d = 12.7 Å (1.3 nm) indicating domains with lower HDTMA intercalation. The SEM/EDX analysis confirmed the composition of organically modified vermiculites by enumeration of elements.

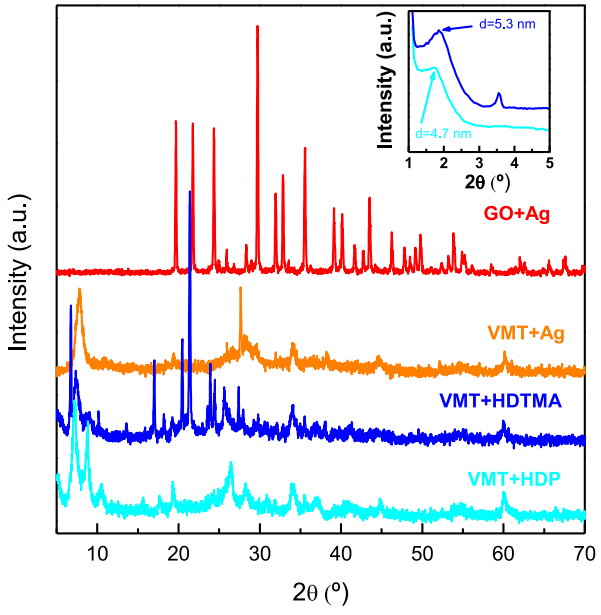

Fig. 2. XRD patterns of modified fillers.

3.2. Antimicrobial properties of fillers

The antimicrobial effect of the fillers was evaluated by two independent methods including MIC determination in the liquid medium and disk diffusion method [45,46]. The pure fillers of GO and VMT were used as a negative control, for which no antimicrobial effect was found. The MIC results of GO + Ag and VMT + Ag were compared with MIC of $AgNO_3$. Table 2 summarizes the MIC values obtained for each sample against the tested microorganisms. It is clearly observed that G-strains are more sensitive to Ag^+ ions than G+ strains [51–53]. The MIC values of GO + Ag for *E. coli* and *P. aeruginosa* were only slightly higher than for $AgNO_3$, i.e., the antibacterial effect was reduced relatively little ($p > 0.05$). However, the MIC for *S. aureus* and *S. salivarius* bacterial strains and the yeast *C. albicans* are almost identical to those for $AgNO_3$ ($p > 0.05$). These results indicate that the antimicrobial activity of silver remains sufficiently preserved after binding to GO.

The VMT + Ag filler showed a lower antimicrobial effect for G- (5 ×) and G+ (almost 2 ×) bacteria than GO + Ag ($p < 0.05$). This difference can be explained by the much lower content of silver in VMT + Ag than in GO + Ag, as was determined by ICP-AES method, but also by the differences in the structure of both composites. While in GO + Ag, the silver is attached mainly to the surface of GO, in VMT + Ag it can be also intercalated between the layers. The antibacterial substances HDP and HDTMA have a stronger antimicrobial effect against G+ bacteria (MIC = 0.5 μg/mL) than against G- *E. coli* (MIC = 1.5 μg/mL). These differences are probably due to the binding mechanism of these substances to the structurally different surface membranes of G+ and G-bacteria [51,52,54,55]. In the case of *P. aeruginosa*, the high MIC values obtained indicate that this strain is almost resistant to them (MIC ≥50 μg/mL, $p < 0.05$) [56]. *C. albicans* yeast had MIC = 1.0 μg/mL for both substances. The work of Araujo et al. [57] reported a value 0.75 μg/mL for HDP against yeast, which is a similar value as here. After binding of the HDP and HDTMA to VMT, the sensitivity to the evaluated substances decreased for all bacterial strains and yeasts about 10 times ($p < 0.05$).

The susceptibility of bacteria and yeast to fillers was then evaluated by disk diffusion method by measuring the size of the inhibition zones (Figs. 3 and 4). Samples were applied to the discs in a concentration range of 37, 74, 111, 148 μg/disc (see Table S5). The results of GO + Ag and VMT + Ag show a significant inhibitory effect for all bacterial strains, with a slight concentration dependence (see Fig. 3). Similar results of the antibacterial effect of GO + Ag against *E. coli* and *S. aureus* were reported by Liu et al. [58]. The weakest inhibitory effect was found against the yeast *C. albicans*. These results fully correspond to the MIC results (see Table 2).

Evaluation of VMT + HDP and VMT + HDTMA fillers confirmed higher activity against G+ than G-bacteria, in both procedures. The inhibition zones of *S. aureus* and *S. salivarius* increased with the sample concentration. The antibacterial effect of VMT + HDP against *E. coli* was manifested only from concentrations higher than 111 μg/disc, while in the case VMT + HDTMA was from the concentration higher than 74 μg/disc. These results are consistent with the MIC results, where *P. aeruginosa* was almost resistant, the MIC value of *E. coli* was higher (3x) than that of the G+ bacteria, and *C. albicans* was also inhibited, although it was more resistant to GO + Ag and VMT + Ag.

The evaluation of activity showed that fillers are a suitable material for providing antimicrobial effects. After binding, the antimicrobial effect of Ag, HDP and HDTMA remains at an acceptable level, which is a necessary prerequisite for their further use.

3.3. Polymeric composites

The neat PLA was mixed with the prepared antimicrobial fillers GO + Ag, VMT + Ag, VMT + HDP and VMT + HDTMA. The content of each

Table 2
MIC values of GO + Ag, VMT + Ag, VMT + HDP, VMT + HDTMA, HDP, HDTMA and $AgNO_3$ samples.

Strain	MIC (μg/mL)						
	GO + Ag	VMT + Ag	$AgNO_3$	VMT + HDP	VMT + HDTMA	HDP	HDTMA
E. coli	15	75	10	15	15	1.5	1.5
P. aeruginosa	15	75	10	>500	>500	>50	>50
S. aureus	160	300	160	5	5	0.5	0.5
S. salivarius	160	300	160	5	5	0.5	0.5
C. albicans	160	300	160	10	10	1	1

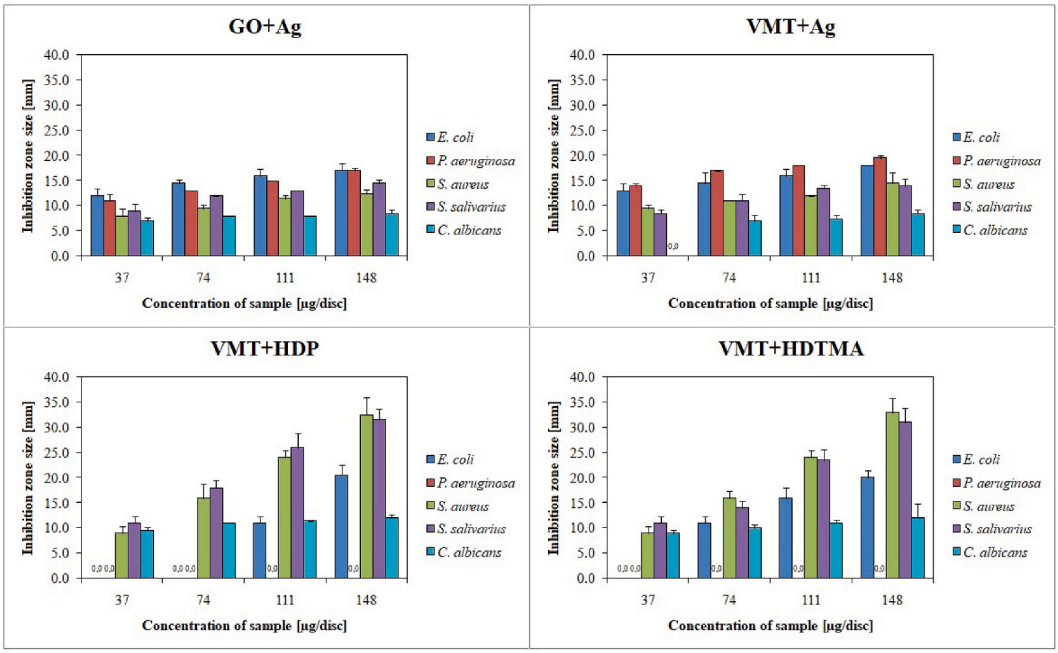

Fig. 3. Average inhibition zones (mm) of modified fillers.

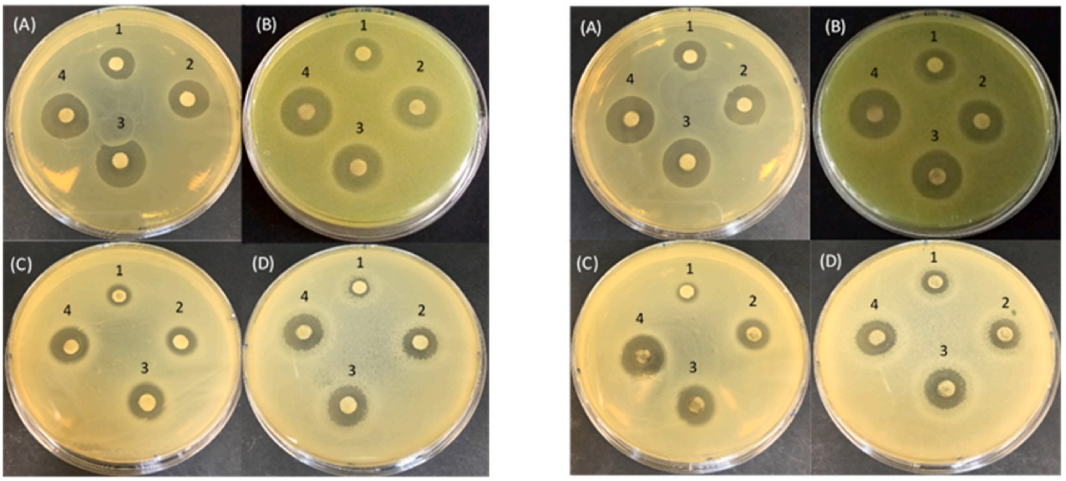

Fig. 4. Antibacterial activities of GO + Ag (left) and VMT + Ag (right) samples against strains *E. coli* (A), *P. aeruginosa* (B), *S. aureus* (C), *S. salivarius* (D). Numbers 1–4 indicate the tested concentration of the samples: n° 1 = 37 μg/disc; n° 2 = 74 μg/disc; n° 3 = 111 μg/disk; n° 4 = 148 μg/disc.

filler in the composite was 1 wt%, see Table 1. These polymer composites were further characterized by XRD, DSC and TGA to describe their structural and thermal properties. The thus prepared and characterized composites were immersed in physiological solutions of pH 7 or 9 at a temperature of 37 °C for a specified period of 1, 2, 3 and 6 months. Changes in their structure and morphology were monitored using SEM and optical microscopy, and antimicrobial tests were also performed. The main objective of this study was to observe how the antibacterial properties of the composites change over time with respect to the integrity of the composite.

The XRD patterns of the neat PLA and PLA composites are shown in Fig. 5. It can be seen that they are characterized by a broad halo (i.e. 2θ

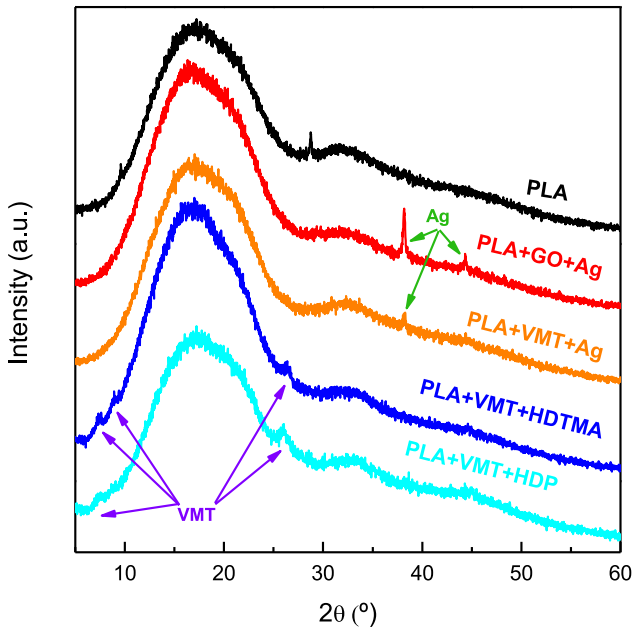

Fig. 5. XRD profiles of PLA and its composites with modified fillers.

range of between 10° and 26°) and some small diffraction peaks. The small diffraction peaks at 2θ = 9.5° and 28.7° are attributed to α-polymorph of the PLA. The PLA composites with silver-fillers exhibit reflections at around 38° (111), and 44° (200), corresponding to the presence of silver nanoparticles. In the case of organo-vermiculite fillers, the apparition of reflections at 7.3°, 8.8° and around 26.2°, corresponding to modified clay minerals, is also appreciated. These patterns pointed out the existence of a low degree of crystallinity. The neat PLA and PLA composites were therefore more amorphous materials with increased degradation capability suitable for the intended testing of long-term antimicrobial activity [1].

Thermal properties of the neat PLA and the PLA composites were determined using DSC and TGA measurements to see the influence of fillers in the PLA matrix. The values of glass transition temperature (T_g), the cold crystallization temperature (T_{cc}) and the melting temperature (T_m) along with the enthalpy of each process are determined by DSC and are collected in Table 3 and displayed in Fig. 6. The degree of crystallinity (X_c) was also included and is calculated by subtracting the enthalpy of crystallization (ΔH_{cc}) from the melting enthalpy (ΔH_m) and dividing it by the enthalpy fusion corresponding to a single PLA crystal ($\Delta H_f = 93.6$ J/g) [59].

The physical aging of the materials is easily distinguished, the T_g of PLA is determined around 59 °C. Furthermore, in the composites, the incorporation of silver-fillers slightly increases T_g; being the highest the PLA + GO + Ag composite. This is due to the higher amount of silver

Table 3
DSC results of the neat PLA and its composites.

Sample	T_g (°C)	T_{cc} (°C)	ΔH_{cc} (%/°C)	T_m (°C)	ΔH_m (%/°C)	X_c (%)
PLA	59.0	101.0	29.0	152.0	30.0	1.1
PLA + GO + Ag	59.5	109.5	30.5	153.0	34.5	3.2
PLA + VMT + Ag	59.5	109.5	29.0	152.0	32.0	3.2
PLA + VMT + HDTMA	58.5	100.0	45.5	153.0	51.5	6.4
PLA + VMT + HDP	59.0	101.5	31.0	153.5	34.5	3.7

Standard errors (±): 1 °C for temperatures, 1% in ΔH_m and 5% for X_c.

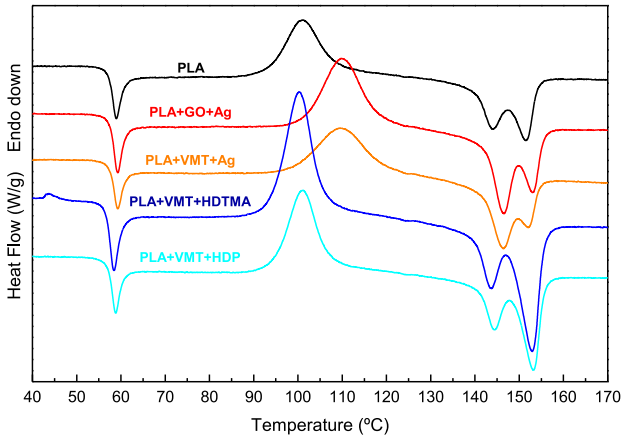

Fig. 6. DSC curves of PLA and its composites.

particles in GO in comparison to those incorporated in vermiculites. However, this temperature increment is practically tenuous when HDP is introduced into the structure; that is, the T_g of PLA + VMT + HDP is similar to neat PLA. The opposite case occurs when vermiculite with HDTMA is incorporated due to the higher flexibility of HDTMA compared to HDP as well as the higher percentage of cation exchange produced in the vermiculite. The silver-filler effect is also observed for T_{cc}, where a shift to higher temperatures was identified compared to the neat PLA or PLA containing organically modified vermiculites. In the melting process, two peaks were visible in all cases, including the neat PLA. These are attributed to the occurrence of several crystalline polymorphs, α- and α′-form [60,61]. The first one corresponds to the melting of small and imperfect crystallites in the amorphous part of PLA matrix, which melt first and evolve to higher perfection structure in α-phase [62]. The incorporation of silver-filler provokes an increase of less perfect lattices with respect to the α-form, but higher crystallinity and also crystal perfection with a higher T_m. The organically modified vermiculite fillers act as nucleating agent increasing crystallinity and the α-form formation with a slightly increase in melting temperature. Despite this, the crystallinity is very low in all systems as observed in the XRD patterns.

A thermogravimetric analysis was performed to determine the thermal stability of the composites. The initial thermal degradation (T_i) was taken as 5% mass loss and the temperature at the maximum weight loss (T_{max}) was determined using the corresponding derivative curves (DTG). The resulting data are collected in Table 4.

The thermal degradation under argon atmosphere in the case of the neat PLA took place in one step, with a maximum at 366.0 °C (see Fig. 7). In the case of composites, the behavior is quite similar except for PLA + VMT + HDTMA, which presents a lower temperature possibly due to the presence of long-chain organics in the filler, being, also, in higher amount compared to PLA + VMT + HDP, and which have lower thermal stability [26].

Table 4
TGA values for the neat PLA and PLA composites.

Samples	Ti (°C)	Tmax (°C)	-dW/dT (wt%/°C)
PLA	331	366.0	34.0
PLA + GO + Ag	331	364.5	30.5
PLA + VMT + Ag	333	366.0	33.0
PLA + VMT + HDTMA	322	366.0	31.5
PLA + VMT + HDP	333	365.5	31.0

Standard errors (±): 1 °C for temperatures and 1% for weight.

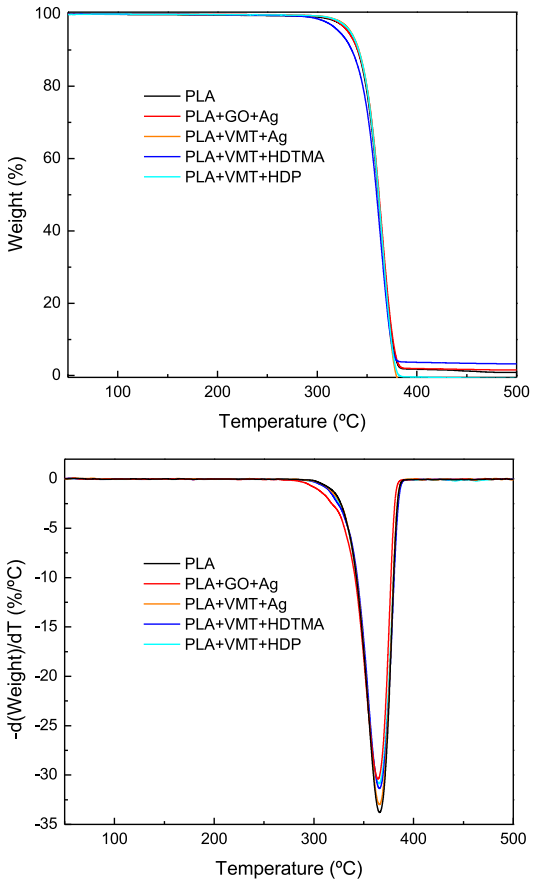

Fig. 7. TGA and DTG curves of PLA and its composites.

3.4. Antimicrobial tests after immersion in physiological pHs

The qualitative analysis of the sample physical integrity and erosion processes that took place during immersion at different pH and at 37 °C was monitored using scanning electron microscopy and optical microscopy. Figs. 8 and 9 show SEM and optical microscopy of the PLA and composites at different times and pHs. The neat PLA was initially transparent, after immersion in saline buffers the polymer acquired a milky color and its physical and mechanical stability visibly deteriorated. This was taken as an apparent evidence of the degradation changes that had occurred, since the deterioration of the physical and mechanical properties of PLA (in that case, brittleness) is precisely due to hydrolytic degradation. It is well known, that hydrolysis of the amorphous regions of PLA occurs more easily due to the less organized structure than the crystalline ones and thus leads to an increase in the crystallinity of the hydrolyzed polymer and a decrease in the quality of mechanical and physical properties [1,41]. Here, it was found that while the samples that were immersed for 1–2 months retained their integrity, after three months of immersion at different pHs, they showed a much higher brittleness leading to a tendency to disintegrate after 6 months of immersion in the solutions.

SEM analysis and optical microscopy were performed to monitor morphological changes on the polymer surface (Fig. 8). Surface changes were more noticeable in optical microscope images. A slight disruption of the structure was confirmed at 3 months but was more visible at 6 months. The effect of pH 9 on this deterioration was more accused. Weighing on five-digit analytical balances, it was found that the change in the weight of the samples after 6 months reached a decrease of 10% at both pH. In general, PLA undergoes hydrolytic cleavage in the presence of water based on bimolecular nucleophilic substitution, and this

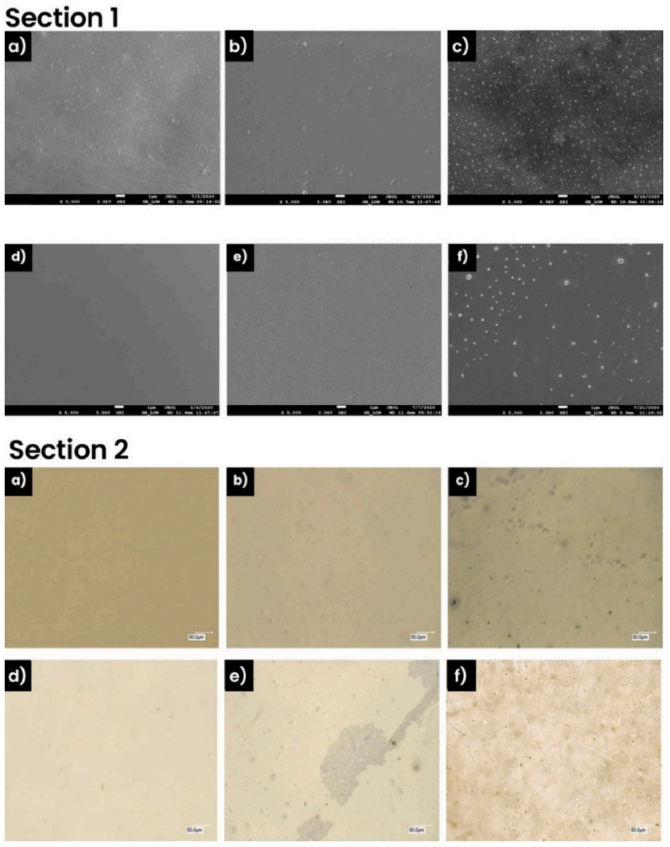

Fig. 8. Section 1 - SEM images of the neat PLA: magnification 5000 × , pH = 7 at a) 0 months, b) 3 months, c) 6 months; pH = 9 at time: d) 0 months, e) 3 months, f) 6 months. Section 2 - Optical microscope images of PLA: magnification 500 × , pH = 7 at a) 0 months, b) 3 months, c) 6 months; pH = 9 at d) 0 months, e) 3 months, f) 6 months.

reaction is catalyzed by acids or bases. Under alkaline conditions, oligomeric acids dissociated into $RCOO^-$ are formed being more hydrophilic than non-dissociated RCOOH oligomers formed under neutral conditions. $RCOO^-$ ions diffuse from the PLA sample into external solutions much more easily than RCOOH, which accelerates PLA degradation [1, 63–71].

Hydrolysis is part of a multi-step degradation process called erosion. Visually, it was found that mainly a bulk erosion took place, as the samples retained their size and shape, but at the same time there was a partial loss of strength and structural integrity [39,71].

As can be observed in Fig. 9A and B, the composites underwent more obvious structural changes in the 0-6-month period than the neat PLA. However, there was a clear difference between PLAs bearing the silver fillers and PLAs containing organovermiculites. The ones with silver-fillers were gray-brown in color at first and then turned to an opaque dark gray. The PLA + VMT + HDP and PLA + VMT + HDTMA showed similar milky color as the degraded neat PLA. SEM analysis showed a visible alteration in the morphology of the composite after 3 months, which was more evident after 6 months, when delamination, cracks and voids appeared in the surface films. The most significant structure alteration was visible in the case of PLA + VMT + HDTMA composite at alkaline pH, which is consistent with [71] although the weight loss after 6 months was only about 10%.

Like the neat PLA, the composites showed deteriorated mechanical properties after three months of immersion. Their brittleness has increased. After 6 months of immersion, they tended to disintegrate when removed from the solution, although they appeared intact and the same size and shape as at the beginning (0 month). Despite these changes, all composites were still useable for microbiological tests.

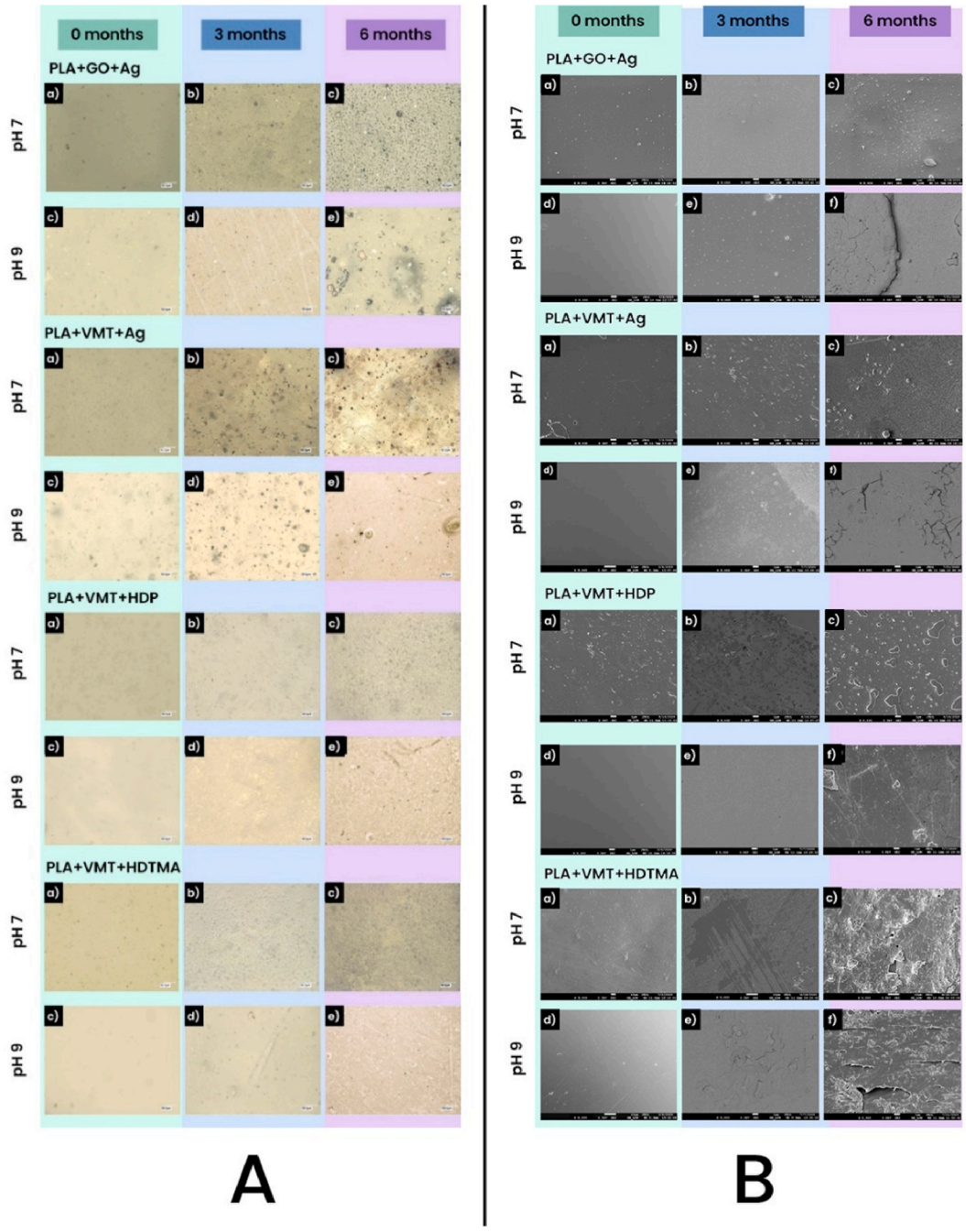

Fig. 9. A: Optical microscopy images of polymer composites, magnification 500 × : PLA + GO + Ag, pH = 7 at a) 0 months, b) 3 months, c) 6 months; pH = 9 at time d) 0 months, e) 3 months, f) 6 months; PLA + VMT + Ag, pH = 7 at time a) 0 months, b) 3 month s, c) 6 months; pH = 9 at time d) 0 months, e) 3 months, f) 6 months; PLA + VMT + HDP, pH = 7 at time a) 0 months, b) 3 months, c) 6 months; pH = 9 at time d) 0 months, e) 3 months, f) 6 months; PLA + VMT + HDTMA pH = 7 at time a) 0 months, b) 3 months, c) 6 months; pH = 9 at time d) 0 months, e) 3 months, f) 6 months. B: SEM images of polymeric composites, magnification 5000 × : PLA + GO + Ag, pH = 7 at time a) 0 months, b) 3 months, c) 6 months; pH = 9 at time d) 0 months, e) 3 months, f) 6 months; PLA + VMT + Ag, pH = 7 at time a) 0 months, b) 3 months, c) 6 months; pH = 9 at time d) 0 months, e) 3 months, f) 6 months; PLA + VMT + HDP, pH = 7 at time a) 0 months, b) 3 months, c) 6 months; pH = 9 at time d) 0 months, e) 3 months, f) 6 months; PLA + VMT + HDTMA pH = 7 at time a) 0 months, b) 3 months, c) 6 months; pH = 9 at time d) 0 months, e) 3 months, f) 6 months.

Due to these changes in the above-named properties, it was clear that degradation, that there was degradation, probably bulk erosion, but we do not precisely distinguish between bulk and surface erosion [42]. In case of PLA + GO + Ag and PLA + VMT + Ag, the presence of hydrophilic fillers in the PLA matrix promotes the rate of hydrolytic degradation of the polymer due to reduced interfacial adhesion between the filler and the matrix. It is also associated with a homogeneous distribution in the polymer matrix. If the filler is not completely homogeneously distributed in the matrix, it may be easier to disrupt the PLA structure. It is clear from Fig. 9A, that distribution of fillers in PLA + GO + Ag and PLA + VMT + Ag was not ideal but fine. On the other hand, organovermiculites used were hydrophobic and were homogeneously distributed in the PLA matrix. However, after 6 months of immersion, the surface degradation is most visible, especially in the case of the PLA + VMT + HDTMA, see Fig. 9 [2,72,73].

All composites were also subjected to elemental SEM/EDX analysis

after 6 months to determine the presence of Ag or Si, as Si is the main component of vermiculite. Fig. 10 confirmed the presence of Ag visible as red clusters on the surface of PLA + GO + Ag and PLA + VMT + Ag, and in the case of the PLA + VMT + HDP and PLA + VMT + HDTMA, the presence of silicon (in green) is identified on the surface. The silver content is visibly lower in the case of PLA + VMT + Ag than that of PLA + GO + Ag, which is consistent with the ICP-AES analyses.

Antimicrobial testing of all PLA composites was performed in the same manner as for the neat PLA polymers. The PLA + GO and PLA + VMT composites which had no inhibitory effects on the tested microorganisms, were used as negative controls. In the case of silver-containing composites, the differences between the type of GO and VMT fillings were evaluated. The results for all 5 strains are included in the heat analysis map (see Fig. 11).

It was found that for PLA + GO + Ag, depending on the immersion time, there is a slightly increased inhibitory effect for all bacterial strains, but not for the *C. albicans* yeast, where it is null. The antibacterial effect of PLA + GO + Ag composite was also demonstrated in a study by Liu et al. [58] or in Ref. [74]. The effect of alkaline pH on the increase of inhibition growth is not significant for PLA + GO + Ag ($p > 0.05$), except for *P. aeruginosa* and *S. aureus* strains after 6 months. In the case of PLA + VMT + Ag, in addition to immersion time, the alkaline pH also contributed to the increase in inhibition after 6 months ($p < 0.05$), with the exception of *S. salivarius* strain. It corresponds to the larger visible changes on the PLA + VMT + Ag surface at pH 9 than at pH 7 (see Fig. 9). This could lead to a better diffusion of silver into the disc environment. A comparison of the antimicrobial effects of both composites showed an overall weaker inhibitory effect of PLA + VMT + Ag compared to PLA + GO + Ag ($p < 0.05$). While PLA + GO + Ag had inhibition effect throughout the tested time at both pHs, PLA + VMT + Ag only after the first month of immersion. However, after 3 months of the experiments, the inhibition effects of both composites were comparable, in some cases the effects of PLA + VMT + Ag were higher. The earlier antimicrobial effect of PLA + GO + Ag was probably due to the much higher content of Ag species, especially Ag^{+}, in GO + Ag than in VMT + Ag and the different anchoring of silver particles on GO and VMT.

In the case of PLA + VMT + HDP and PLA + VMT + HDTMA composites, the effect of immersion time on the deterioration of PLA composites is clearly visible in all strains, including yeast ($p < 0.05$). For both composites, pH 9 has a more positive effect on the inhibitory effect. A higher sensitivity to G+ strains, especially *S. aureus,* was detected. Related to G-strains, PLA + VMT + HDP was effective only after 3 months of immersion, PLA + VMT + HDTMA even after 6 months. The results correspond to our previous MIC results [75], when VMT + HDP an VMT + HDTMA were effective against G+ bacteria (*S. aureus and S. salivarius)*, however they were no efficient against G- (*E. coli and P. aeruginosa*). VMT + HDP appeared to be more effective than VMT + HDTMA [75]. Based on these results, it can be assumed that at pH 9, which is in the gallbladder, the surface alteration of the material can slightly accelerate and/or increase the release of antimicrobials into the environment. The lower degradation effect is related to the good homogenization of fillers in the PLA matrix and the fact that the surface of PLA composites with organovermiculites is more hydrophobic, thus their release to the aqueous environment may not be as supported as in the case of inorganic fillers. In our previous study, the poorer stability of vermiculite modified by HDP cations in acidic and alkaline environment compared to vermiculite modified by HDTMA cations was confirmed [28]. It can be assumed that after 6 months at pH = 9, the vermiculite structure was slightly degraded and HDP cations were probably more

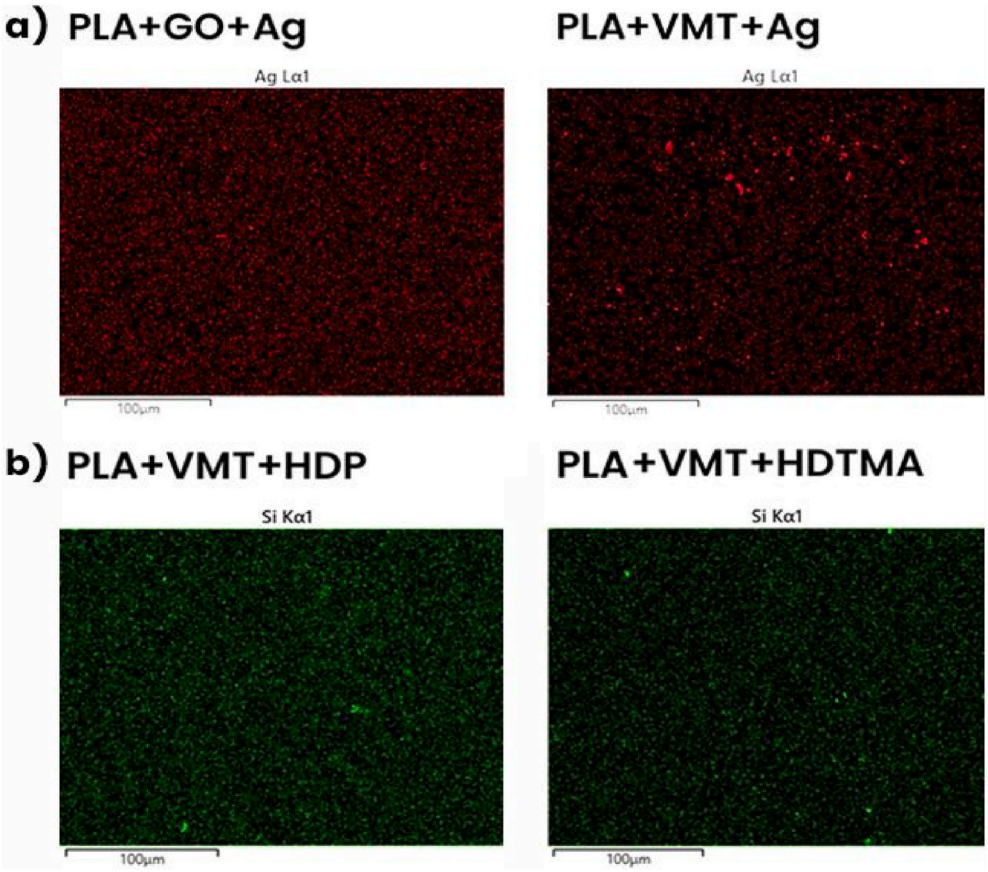

Fig. 10. a) SEM/EDX analysis to confirm the presence of Ag (red dots) in PLA + GO + Ag and PLA + VMT + Ag samples, b) SEM/EDX analysis to confirm the presence of Si (green dots) in PLA + VMT + HDP and PLA + VMT + HDTMA samples. (For interpretation of the references to color in this figure legend, the reader is referred to the Web version of this article.)

Samples	Composite Time	*Escherichia coli*		*Pseudomonas aeruginosa*		*Staphylococcus aureus*		*Streptococcus salivarius*		*Candida albicans*	
		pH 7	pH 9	pH 7	pH 9	pH 7	pH 9	pH 7	pH 9	pH 7	pH 9
PLA+GO+Ag	0 M	7.9	8.0	14.4	14.4	9.3	9.3	9.0	9.0	0.0	0.0
	1 M	9.4	11.0	13.8	13.7	9.1	10.1	9.4	10.7	0.0	0.0
	2 M	10.3	10.2	14.1	14.2	12.9	12.0	12.1	13.0	0.0	0.0
	3 M	10.1	12.0	14.5	17.0	10.7	11.2	12.0	11.0	0.0	0.0
	6 M	13.8	13.8	17.3	21.1	14.0	19.0	8.0	8.0	0.0	0.0
PLA+VMT+Ag	0 M	0.0	0.0	0.0	0.0	0.0	0.0	0.0	0.0	0.0	0.0
	1 M	0.0	0.0	0.0	0.0	0.0	0.0	0.0	0.0	0.0	0.0
	2 M	7.6	8.0	9.2	15.2	9.3	12.4	8.3	8.5	0.0	0.0
	3 M	11.9	10.0	10.9	24.3	11.7	13.4	8.8	8.8	0.0	0.0
	6 M	11.6	16.3	17.2	28.1	12.6	15.5	11.1	12.6	0.0	0.0
PLA+VMT+HDP	0 M	0.0	0.0	0.0	0.0	9.9	9.9	12.8	12.8	0.0	0.0
	1 M	0.0	0.0	0.0	0.0	10.0	9.5	10.8	10.6	0.0	0.0
	2 M	0.0	0.0	0.0	0.0	10.4	11.4	11.6	13.6	0.0	0.0
	3 M	9.8	10.0	10.9	18.1	12.4	13.3	11.3	10.6	0.0	0.0
	6 M	11.2	12.1	18.1	18.9	20.0	31.0	13.8	24.2	12.3	20.8
PLA+VMT+HDTMA	0 M	0.0	0.0	0.0	0.0	12.9	12.9	8.8	8.8	0.0	0.0
	1 M	0.0	0.0	0.0	0.0	10.0	10.5	9.8	9.8	0.0	0.0
	2 M	0.0	0.0	0.0	0.0	10.1	11.0	12.1	13.0	0.0	0.0
	3 M	0.0	0.0	0.0	0.0	12.4	11.3	12.3	11.7	0.0	0.0
	6 M	9.9	14.0	10.9	18.1	12.4	15.7	12.2	15.7	0.0	0.0

Fig. 11. Heat map analysis of PLA composites (discs) for microbial strains based on average of inhibition zone (mm). PLA composites immersed for 0, 1, 2, 3 and 6 months in saline solution at pH = 7 and 9. All sorts of color in figure represents the size of the inhibition zones, red indicates the largest average of the inhibition zone, green represents the minimal average of the inhibition zone. (For interpretation of the references to color in this figure legend, the reader is referred to the Web version of this article.)

accessible to the tested strains and strongly inhibit their growth.

The main goal of this study was to observe the long-term antimicrobial effect of PLA composites after immersion at different pHs for a given time. No other parameters besides antimicrobial activities and visual evaluation were monitored. We worked with small amounts of solutions and small dimensions of composites, thus analyses of silver, organic cations, all PLA oligomer or monomer were not possible due to limited amounts of solutions and limits of detections of analytical instruments. As when working with composites, we wanted to avoid any contamination, so only antimicrobial activity was observed.

In this study, we confirmed our hypothesis about the long-term effects of the PLA composites. Changes in the antimicrobial effect of PLA composites showed that possible degradation of composites occurs slowly, which is manifested by the gradual release of antimicrobial substances from the composite. This effect is medically significant, as it can be used in the prevention of an unwanted inflammation process, and can thereforebe considered an important characteristic in the case of potential application in the medical practice.

4. Conclusion

PLA has been frequently studied for use in biomedical applications due to its mechanical strength, bioresorbability and biocompatibility in the human body. In this study, PLA composites with four fillers with proven antimicrobial properties were prepared and characterized with respect to their antimicrobial character for possible use in the production of medical stents. For the preparation of PLA + GO + Ag, PLA + VMT + Ag, PLA + VMT + HDTMA and PLA + VMT + HDP composites, GO + Ag, VMT + Ag, VMT + HDP and VMT + HDTMA were used as fillers in an amount of 1 wt%. First, the fillers were characterized using XRD, FTIR, SEM/EDX, TOC, ICP/AES methods, especially to confirm their composition. The antimicrobial effect of the fillers was evaluated by two independent methods including MIC determination in liquid medium and disk diffusion method using *E. coli, S. salivarius, S. aureus, P. aeruginosa* and *C. albicans*. A significant inhibitory effect for all bacterial strains was found for GO + Ag and VMT + Ag and a weak inhibitory effect was found against the yeast *C. albicans*. Higher activity against G+ than G-bacteria was confirmed for VMT + HDP and VMT + HDTMA fillers as well as against *C. albicans*. The prepared polymer composites were characterized for their structural and thermal properties. Mainly, their physical integrity was qualitatively monitored during immersion at different pH (7 and 9) at 37 °C for 0–6 months using SEM and optical microscopy together with antimicrobial activity. Microscopic analyses confirmed that damage to all composite surfaces increased with immersion time and was also more visible at pH = 9 than at pH = 7. This was also confirmed by increasing antimicrobial properties over time. In general, after six months of immersion the composites showed the highest antibacterial activity against the tested antimicrobial strains, but only PLA + VMT + HDP was also effective against *C. albicans*. The results confirmed our initial hypothesis that PLA composites, even those which had no effects on microbial organisms after preparation, lose their surface integrity during aging in solutions with different pH allowing to antimicrobial fillers being active. Fillers can reach the surface of the composites and act on the microbial organisms present, or they can prevent the colonization of the composite surface by these microorganisms. This shows the suitability of PLA-based composites for biomedical purposes, e.g. for use as stents or implants, from which an antimicrobial filler or drug can be gradually released.

Funding

This study was supported by the project no. CZ.02.1.01/0.0/0.0/17_049/0008441 “Innovative Therapeutic Methods of Musculoskeletal System in Accident Surgery” within the MSMT Operational program Research, development and education financed by the European Union, by the project LINKA20364 “Design of novel antimicrobial biobased materials using supercritical fluids processes” financed by CSIC and by the project no. CZ.02.2.69/0.0/0.0/19_073/0016945 within the MSMT Operational Programme Research, Development and Education, under project DGS/INDIVIDUAL/2020-001 ″Development of antimicrobial biobased polymeric material using supercritical fluid technology".

Author statement

Kateřina Škrlová – preparation of fillers and composites, characterization of products, preparation of antimicrobial tests, evaluation of the results, preparation of the manuscript, **Zuzana Rybková** – responsible for antimicrobial tests, evaluation of the results, preparation of the manuscript, **Tereza Stachurová** – performance of antimicrobial tests, evaluation of the results, **Jakub Zagora** - characterization of products, preparation of antimicrobial tests, **Kateřina Malachová** – methodology and supervisor of antimicrobial tests, evaluation of the results, preparation of the manuscript, **Dagmar Měřinská** – preparation and characterization of polymer composites, **Roman Gabor** – preparation of SEM and microscopy analyses, **Miroslav Havlíček** – preparation of the manuscript, **Alexandra Muñoz-Bonilla** – supervisor of polymer chemistry and properties, **Marta Fernández-García** - supervisor of polymer chemistry, properties and characterization, evaluation of the results,

preparation of the manuscript, **Daniela Plachá** – responsible of the study, supervisor of all activities, evaluation of the results, preparation of the manuscript.

Declaration of competing interest

The authors declare that they have no known competing financial interests or personal relationships that could have appeared to influence the work reported in this paper.

Data availability

Data will be made available on request.

Acknowledgement

The authors thank Sylva Holešová, PhD, for performing TGA and DSC analyzes, and Marianne Hundáková, PhD. for performing XRD analyzes.

Appendix A. Supplementary data

Supplementary data to this article can be found online at https://doi.org/10.1016/j.polymertesting.2022.107760.

References

[1] S. Teixeira, K.M. Eblagon, F. Miranda, R. Pereira, F. M, J.L. Figueiredo, Towards controlled degradation of poly(lactic) acid in technical applications, 7, 2021, p. 42, https://doi.org/10.3390/c7020042.
[2] Moataz A. Elsawy, Ki-Hyun Kim, Jae-Woo Park, Akash Deep, Hydrolytic degradation of polylactic acid (PLA) and its composites, Renew. Sustain. Energy Rev. 79 (2017) 1346–1352, https://doi.org/10.1016/j.rser.2017.05.143. ISSN 1364-0321.
[3] K. Škrlová, K. Malachová, A. Muñoz-Bonilla, D. Měřinská, Z. Rybková, M. Fernández-García, D. Plachá, Biocompatible polymer materials with antimicrobial properties for preparation of stents, Nanomaterials [online] 9 (11) (2019), https://doi.org/10.3390/nano9111548. ISSN 20794991.
[4] L.-T. Lim, R. Auras, M. Rubino, Processing technologies for poly(lactic acid), Prog. Polym. Sci. 33 (Issue 8) (2008) 820–852, https://doi.org/10.1016/j.progpolymsci.2008.05.004. ISSN 0079-6700.
[5] K. Rojas, D. Canales, N. Amigo, L. Montoille, A. Cament, L.M. Rivas, O. Gil-Castell, P. Reyes, M.T. Ulloa, A. Ribes-Greus, et al., E_ective antimicrobial materials based on low-density polyethylene (LDPE) with zinc oxide (ZnO) nanoparticles, Compos. B Eng. 172 (2019) 173–178.
[6] H. Liu, W. Song, F. Chen, L. Guo, J. Zhang, Interaction of microstructure and interfacial adhesion on impact performance of polylactide (PLA) ternary blends, Macromolecules 44 (2011) 1513–1522.
[7] A. Góra, D. Pliszka, S. Mukherjee, S. Ramakrishna, Tubular tissues and organs of human body—Challenges in regenerative medicine, J. Nanosci. Nanotechnol. 16 (2016) 19–39, https://doi.org/10.1166/jnn.2016.11604.
[8] X. He, W. Fu, J. Zheng, Cell sources for trachea tissue engineering: past, present and future, Regen. Med. 7 (2012) 851–863, https://doi.org/10.2217/rme.12.96.
[9] S. McMahon, N. Bertollo, E.D.O. Cearbhaill, J. Salber, L. Pierucci, P. Duffy, T. Dürig, V. Bi, W. Wang, Bio-resorbable polymer stents: a review of material progress and prospects, Prog. Polym. Sci. 83 (2018) 79–96, https://doi.org/10.1016/j.progpolymsci.2018.05.002.
[10] T.R. Welch, A.W. Nugent, S.R. Veeram Reddy, Biodegradable stents for congenital heart disease, Interv. Cardiol. Clin. 8 (2019) 81–94, https://doi.org/10.1016/j.iccl.2018.08.009.
[11] J. Laukkarinen, I. Nordback, J. Mikkonen, P. Kärkkäinen, J. Sand, A novel biodegradable biliary stent in the endoscopic treatment of cystic-duct leakage after cholecystectomy, Gastrointest. Endosc. 65 (2007) 1063–1068, https://doi.org/10.1016/j.gie.2006.11.059.
[12] J. Laukkarinen, J. Sand, J. Leppiniemi, M. Kellomäki, I. Nordback, A novel technique for hepaticojejunostomy for nondilated bile ducts: a purse-string anastomosis with an intra-anastomotic biodegradable biliary stent, Am. J. Surg. 200 (2010) 124–130, https://doi.org/10.1016/j.amjsurg.2009.05.012.
[13] G. Ginsberg, C. Cope, J. Shah, T. Martin, A. Carty, P. Habecker, C. Clerc, J.-P. Nuutinen, P. Törmälä, In vivo evaluation of a new bioabsorbable self-expanding biliary stent, Gastrointest. Endosc. 58 (2003) 777–784, https://doi.org/10.1016/S0016-5107(03)02016-9.
[14] X. Xu, T. Liu, S. Liu, K. Zhang, Z. Shen, Y. Li, X. Jing, Feasibility of biodegradable PLGA common bile duct stents: an in vitro and in vivo study, J. Mater. Sci. Mater. Med. 20 (2009) 1167–1173, https://doi.org/10.1007/s10856-008-3672-2.
[15] T.-F.C. Mah, G.A. O'Toole, Mechanisms of biofilm resistance to antimicrobial agents, Trends Microbiol. 9 (2001) 34–39, https://doi.org/10.1016/S0966-842X(00)01913-2.
[16] I. Brook, Aerobic and anaerobic microbiology of biliary tract disease, J. Clin. Microbiol. 27 (10) (1989) 2373–2375.
[17] M. Votava, P. Ondrovčík, Vybrané Kapitoly Z Klinické Mikrobiologie, 1998, ISBN 80-210-1805-4.
[18] W. Levinson, Review of Medical Microbiology and Immunology, twelfth ed., McGraw-Hill Companies, 2012, ISBN 978-0-07-177434-5.
[19] D.J. Sullivan, S. Azlin-Hasim, M. Cruz-Romero, E. Cummins, J.P. Kerry, M. A. Morris, Natural Antimicrobial Materials for Use in Food Packaging, Elsevier Inc., Amsterdam, The Netherlands, 2018. ISBN 9780128119822.
[20] M. Azizi-Lalabadi, H. Hashemi, J. Feng, S.M. Jafari, Carbon nanomaterials against pathogens; the antimicrobial activity of carbon nanotubes, graphene/graphene oxide, fullerenes, and their nanocomposites, Adv. Colloid Interface Sci. 284 (2020), https://doi.org/10.1016/j.cis.2020.102250, 102250, ISSN 0001-8686.
[21] D. Plachá, J. Jampilek, Graphenic materials for biomedical aplications, Nanomateriály 9 (2019) 1758, https://doi.org/10.3390/nano9121758.
[22] N. Li, L. Yu, Z. Xiao, C. Jiang, B. Gao, Z. Wang, Biofouling mitigation effect of thin film nanocomposite membranes immobilized with laponite mediated metal ions, Desalination 473 (114162) (2020), https://doi.org/10.1016/j.desal.2019.114162. ISSN 0011-9164.
[23] C. Loyo, V. Moreno-Serna, J. Fuentes, N. Amigo, F.A. Sepúlveda, J. Ortiz A, L. M. Rivas, M.T. Ulloa, R. Benavente, P.A. Zapata, PLA/CaO nanocomposites with antimicrobial and photodegradation properties, Polym. Degrad. Stabil. 197 (2022), 109865, https://doi.org/10.1016/j.polymdegradstab.2022.109865. ISSN 0141-3910.
[24] M. Yahyaoui, O. Gordobil, R.H. Díaz, M. Abderrabba, J. Labidi, Development of novel antimicrobial films based on poly(lactic acid) and essential oils, React. Funct. Polym. 109 (2016) 1–8, https://doi.org/10.1016/j.reactfunctpolym.2016.09.001. ISSN 1381-5148.
[25] D. Plachá, A. Muñoz-Bonilla, K. Škrlová, C. Echeverria, A. Chiloeches, M. Petr, K. Lafdi, M. Fernández-García, Antibacterial character of cationic polymers attached to carbon-based nanomaterials, Nanomaterials 10 (6) (2020) 1218, https://doi.org/10.3390/nano10061218.
[26] D. Plachá, G.S. Martynková, M. Rümmeli, Variations in the sorptive properties of organovermiculites modified with hexadecyltrimethylammonium and hexadecylpyridinium cations, J. Sci. Conf. Proc. [online] 2 (1) (2010) 36–41, https://doi.org/10.1166/jcp.2010.1006. ISSN 19376456.
[27] D. Plachá, G.S. Martynková, M. Rümmeli, Preparation of organovermiculites using HDTMA: structure and sorptive properties using naphthalene, J. Colloid Interface Sci. [online] 327 (2) (2008) 341–347, https://doi.org/10.1016/j.jcis.2008.08.026. ISSN 00219797.
[28] D. Plachá, G.S. Martynková, A. Bachmatiuk, P. Peikertová, J. Seidlerová, M. Rümmeli, The influence of pH on organovermiculite structure stability, Appl. Clay Sci. 93–94 (2014) 17–22, https://doi.org/10.1016/j.clay.2014.03.008. ISSN 0169-1317.
[29] G. Gosheger, Silver-coated megaendoprostheses in a rabbit model—an analysis of the infection rate and toxicological side effects, Biomaterials 25 (2004) 5547–5556.
[30] S. Maharubin, C. Nayak, O. Phatak, A. Kurhade, M. Singh, Y. Zhou, G. Tan, Polyvinylchloride coated with silver nanoparticles and zinc oxide nanowires for antimicrobial applications, Mater. Lett. 249 (2019) 108–111.
[31] P. Dutta, B. Wang, Zeolite-supported silver as antimicrobial agents, Coord. Chem. Rev. 383 (2019) 1–29.
[32] S. Holešová, M. Hundáková, E. Pazdziora, Antibacterial kaolinite based nanocomposites, Procedia Mater. Sci. 12 (2016) 124–129.
[33] J. Rhim, S. Hong, Ch Ha, Tensile, water vapor barrier and antimicrobial properties of PLA/nanoclay composite films, LWT - Food Sci. Technol. (Lebensmittel-Wissenschaft -Technol.) 42 (Issue 2) (2009) 612–617, https://doi.org/10.1016/j.lwt.2008.02.015. ISSN 0023-6438.
[34] J. Chen, H. Peng, X. Wang, F. Shao, Z. Yuan, H. Han, Graphene oxide exhibits broad-spectrum antimicrobial activity against bacterial phytopathogens and fungal conidia by intertwining and membrane perturbation, Nanoscale 6 (2014) 1879–1889.
[35] K. Nakata, T. Tsuchido, Y. Matsumura, Antimicrobial cationic surfactant, cetyltrimethylammonium bromide, induces superoxide stress in Escherichia coli cells, J. Appl. Microbiol. 110 (2011) 568–579, https://doi.org/10.1111/j.1365-2672.2010.04912.x.
[36] M. Turalija, S. Bischof, A. Budimir, S. Gaan, Antimicrobial PLA films from environment friendly additives, Compos. B Eng. 102 (2016) 94–99, https://doi.org/10.1016/j.compositesb.2016.07.017. ISSN 1359-8368.
[37] H. Li, Z. Wang, H. Zhang, Z. Pan, Nanoporous PLA/(Chitosan nanoparticle) composite fibrous membranes with excellent air filtration and antibacterial performance, Polymers 10 (2018) 1085, https://doi.org/10.3390/polym10101085.
[38] S. Khammassi, M. Tarfaoui, K. Škrlová, D. Měřínská, D. Plachá, F. Erchiqui, Poly (Lactic acid) (PLA)-Based nanocomposites: impact of vermiculite, silver, and graphene oxide on thermal stability, isothermal crystallization, and local mechanical behavior, J. Compos. Sci. 6 (2022) 112, https://doi.org/10.3390/jcs6040112.
[39] N.F. Zaaba, M. Jaafar, A review on degradation mechanisms of polylactic acid: hydrolytic, photodegradative, microbial, and enzymatic degradation, Polym. Eng. Sci. 60 (2020) 2061–2075, https://doi.org/10.1002/pen.25511.
[40] J.C. Middleton, A.J. Tipton, Synthetic biodegradable polymers as orthopedic devices, Biomaterials [online] 21 (23) (2000) 2335–2346, https://doi.org/10.1016/S0142-9612(00)00101-0. ISSN 01429612.
[41] Moataz A. Elsawy, Ki-Hyun Kim, Jae-Woo Park, Akash Deep, Hydrolytic degradation of polylactic acid (PLA) and its composites, Renew. Sustain. Energy

Rev. 79 (2017) 1346–1352, https://doi.org/10.1016/j.rser.2017.05.143. ISSN 1364-0321.
[42] T. Casalini, F. Rossi, A. Castrovinci, G. Perale, A perspective on polylactic acid-based polymers use for nanoparticles synthesis and applications, Front. Bioeng. Biotechnol. 7 (2019) 259, https://doi.org/10.3389/fbioe.2019.00259.
[43] A.S. Niknejad, S. Bazgir, A. Kargari, Mechanically improved superhydrophobic nanofibrous polystyrene/high-impact polystyrene membranes for promising membrane distillation application, J. Appl. Polym. Sci. 138 (2021), e50917, https://doi.org/10.1002/app.50917.
[44] G.F. Brooks, K.C. Carroll, J.S. Butel, S.A. Morse, T.A. Mietzner, Jawetz, Melnick, & Adelberg's Medical Microbiology, 26th Edition, McGraw-Hill Companies, 2013, ISBN 978-0-07-179031-4.
[45] ISO 20776-1, Susceptibility Testing of Infectious Agents and Evaluation of Performance of Antimicrobial Susceptibility Test Devices — Part 1: Broth Micro-dilution Reference Method for Testing the in Vitro Activity of Antimicrobial Agents against Rapidly Growing Aerobic Bacteria Involved in Infectious Diseases, Clinical laboratory testing and in vitro diagnostic test systems, 2019, p. 19.
[46] The European Committee on Antimicrobial Susceptibility Testing and Clinical and Laboratory Standards Institute, Antimicrobial Susceptibility Testing EUCAST Disk Diffusion Method, 2021. https://www.eucast.org/ast_of_bacteria/disk_diffusion_methodology/. (Accessed 1 January 2021).
[47] EUCAST, Disk Diffusion Methodology, 2021. EUCAST: EUCAST [online]. Copyright © [cit. 12.12, https://www.eucast.org/ast_of_bacteria/disk_diffusion_methodology/.
[48] M. Pinto, T.M. Langer, T. Hüffer, T. Hofmann, G.J. Herndl, The composition of bacterial communities associated with plastic biofilms differs between different polymers and stages of biofilm succession, PLoS One 14 (6) (2019), e0217165, https://doi.org/10.1371/journal.pone.0217165.
[49] S.B. Aziz, R.T. Abdulwahid, M.A. Rasheed, O.G. Abdullah, H.M. Ahmed, Polymer blending as a novel approach for tuning the SPR peaks of silver nanoparticles, Polymers 9 (2017) 486, https://doi.org/10.3390/polym9100486.
[50] K. Garg, P. Papponen, A. Johansson, et al., Preparation of graphene nanocomposites from aqueous silver nitrate using graphene oxide's peroxidase-like and carbocatalytic properties, Sci. Rep. 10 (2020) 5126, https://doi.org/10.1038/s41598-020-61929-9.
[51] K. Malachová, P. Praus, Z. Pavlíčková, M. Turicová, Activity of antibacterial compounds immobilised on montmorillonite, Appl. Clay Sci. 43 (3) (2009) 364–368, https://doi.org/10.1016/j.clay.2008.11.003. ISSN 0169-1317.
[52] J. Said, C.C. Dodoo, M. Walker, D. Parsons, P. Stapleton, A.E. Beezer, S. Gaisford, An in vitro test of the efficacy of silver-containing wound dressings against Staphylococcus aureus and Pseudomonas aeruginosa in simulated wound fluid, Int. J. Pharm. 462 (1–2) (2014) 123–128, https://doi.org/10.1016/j.ijpharm.2013.12.037.
[53] S.G.G. Saravia, S.E. Rastelli, C.A. Pineda, H. Palza, M.R. Viera, Antiadhesion and antibacterial activity of silver nanoparticles and graphene oxide-silver nanoparticle composites, Matéria (Rio J.) 25 (2) (2020), https://doi.org/10.1590/s1517-707620200002.1071.
[54] X. Mao, D.L. Auer, W. Buchalla, K.-A. Hiller, T. Maisch, E. Hellwig, A. Al-Ahmad, F. Cieplik, Cetylpyridinium chloride: mechanism of action, antimicrobial efficacy in biofilms, and potential risks of resistance, Antimicrob. Agents Chemother. 64 (2020), https://doi.org/10.1128/AAC.00576-20 e00576-20.
[55] S.Y. Lee, S.Y. Lee, Susceptibility of oral streptococci to chlorhexidine and cetylpyridinium chloride, Biocontrol Sci. 24 (1) (2019) 13–21, https://doi.org/10.4265/bio.24.13.
[56] R.C. Beier, S.L. Foley, M.K. Davidson, D.G. White, P.F. McDermott, S. Bodeis-Jones, S. Zhao, K. Andrews, T.L. Crippen, C.L. Sheffield, T.L. Poole, R.C. Anderson, D. J. Nisbet, Characterization of antibiotic and disinfectant susceptibility profiles among Pseudomonas aeruginosa veterinary isolates recovered during 1994–2003, J. Appl. Microbiol. 118 (2) (2014) 326–342, https://doi.org/10.1111/jam.12707, 96.
[57] H.C. Araujo, L.S. Arias, A.C.M. Caldeirão, L.C.d.F. Assumpção, M.G. Morceli, F. N. de Souza Neto, E.R. de Camargo, S.H.P. Oliveira, J.P. Pessan, D.R. Monteiro, Novel colloidal nanocarrier of cetylpyridinium chloride: antifungal activities on Candida species and cytotoxic potential on murine fibroblasts, J. Fungi 6 (2020) 218, https://doi.org/10.3390/jof6040218.
[58] Ch Liu, J. Shen, K.W.K. Yeung, S.Ch Tjong, Development and antibacterial performance of novel polylactic acid-graphene oxide-silver nanoparticle hybrid nanocomposite mats prepared by electrospinning, ACS Biomater. Sci. Eng. 3 (3) (2017) 471–486, https://doi.org/10.1021/acsbiomaterials.6b00766.
[59] C.S. Lovell, J.M. Fitz-Gerald, C. Park, Decoupling the effects of crystallinity and orientation on the shear piezoelectricity of polylactic acid, J. Polym. Sci., Part B: Polym. Phys. 49 (2011) 1555–1562.
[60] M.A. Cuiffo, J. Snyder, A.M. Elliott, N. Romero, S. Kannan, G.P. Halada, Impact of the fused deposition (FDM) printing process on polylactic acid (PLA) chemistry and structure, Appl. Sci. 579 (2017), https://doi.org/10.3390/app7060579.
[61] Y. Hsieh, S. Nozaki, M. Kido, K. Kamitani, K. Kojio, A. Takahara, Crystal polymorphism of polylactide and its composites by X-ray diffraction study, Polym. J. 52 (2020) 755–763, https://doi.org/10.1038/s41428-020-0343-8.
[62] M.E. Mngomezulu, A.S. Luyt, M.J. John, Morphology, thermal and dynamic mechanical properties of poly(lactic acid)/expandable graphite (PLA/EG) flame retardant composites, J. Thermoplast. Compos. Mater. 32 (1) (2019) 89–107.
[63] H. Tsuji, Y. Ikada, Properties and morphology of poly (L-lactide) 4. Effects of structural parameters on long-term hydrolysis of poly (L-lactide) in phosphate-buffered solution, Polym. Degrad. Stabil. 67 (2000) 179–189.
[64] M. Hakkarainen, Aliphatic Polyesters: Abiotic and Biotic Degradation and Degradation Products Degrad. Aliphatic Polyesters, Springer, 2002, pp. 113–138.
[65] A. Paul, C. Delcourt, M. Alexandre, P. Degée, F. Monteverde, P. Dubois, Polylactide/montmorillonite nanocomposites: study of the hydrolytic degradation, Polym. Degrad. Stabil. 87 (2005) 535–542.
[66] Q. Zhou, M. Xanthos, Nanoclay and crystallinity effects on the hydrolytic degradation of polylactides, Polym. Degrad. Stabil. 93 (2008) 1450–1459.
[67] I. Grizzi, H. Garreau, S. Li, M. Vert, Hydrolytic degradation of devices based on poly (DL-lactic acid) size-dependence, Biomaterials 16 (1995) 305–311.
[68] S. Lyu, D. Untereker, Degradability of polymers for implantable biomedical devices, Int. J. Mol. Sci. 10 (2009) 4033–4065.
[69] A. Göpferich, Mechanisms of polymer degradation and erosion, Biomaterials 17 (1996) 103–114, https://doi.org/10.1016/0142-9612(96)85755-3.
[70] G. Schliecker, C. Schmidt, S. Fuchs, T. Kissel, Characterization of a homologous series of D, L-lactic acid oligomers; a mechanistic study on the degradation kinetics in vitro, Biomaterials 24 (2003) 3835–3844.
[71] M.D. Fernández, M.J. Fernández, Vermiculite/poly(lactic acid) composites: effect of nature of vermiculite on hydrolytic degradation in alkaline medium, Appl. Clay Sci. 143 (2017) 29–38.
[72] S.H. Lee, S. Wang, Biodegradable polymers/bamboo fiber biocomposite with bio-based coupling agent, Compos. Appl. Sci. Manuf. 37 (2006) 80–91.
[73] I. Noda, M.M. Satkowski, A.E. Dowrey, C. Marcott, Polymer alloys of Nodax copolymers and poly (lactic acid), Macromol. Biosci. 4 (2004) 269–275.
[74] Ch Liao, Y. Li, S.Ch Tjong, Antibacterial activities or aliphatic polyester nanocomposites with silver nanoparticles and/or graphene oxide sheets, Nanometerials 9 (2019) 8, 1102.
[75] D. Plachá, K. Rosenbergová, J. Slabotínský, K. Mamulová Kutláková, S. Študentová, G.S. Martynková, Modified clay minerals efficiency against chemical and biological warfare agents for civil human protection, J. Hazard Mater. 271 (2014) 65–72.